Journal of Material Cycles and Waste Management (2023) 25:198–210
https://doi.org/10.1007/s10163-022-01521-7

ORIGINAL ARTICLE

Interactions of operating parameters on the production of waste polypropylene pyrolysis oil: neural fuzzy model and genetic algorithm optimization

Ruming Pan[1] · Marcio Ferreira Martins[2] · Gérald Debenest[1]

Received: 15 December 2021 / Accepted: 3 October 2022 / Published online: 11 October 2022

Abstract
This study aims to maximize the waste polypropylene (WPP) pyrolysis oil yield by regulating the operating parameters. The interactions of operating parameters on the distributions of WPP pyrolysis products were studied comprehensively by the neural fuzzy model. The genetic algorithm was utilized to determine the optimal operating parameters for WPP pyrolysis oil yield. Consequently, the highest oil yield of 68.4 wt% was achieved under 456 °C, 20 min, and 50 mL/min. WPP pyrolysis oil components were characterized by Fourier transform infrared spectroscopy (FTIR) and gas chromatography/mass spectrometry (GC/MS) analyses. The oil was composed of alkenes, alkanes, and naphthenes, with the carbon number ranging from C8 to C34. Lower carrier gas flow rate, shorter residence time, and lower temperature were conducive to forming oil's light fraction. In comparison, higher carrier gas flow rate, longer residence time, and higher temperature resulted in a high oil's heavy fraction production.

Keywords Waste polypropylene · Pyrolysis · Oil yield · Neural fuzzy model · Genetic algorithm

Introduction

Plastic is an indispensable part of modern life due to its price advantage and superior performance [1]. Plastic production has increased by around 239 times between 1950 (1.5 million tons) and 2018 (359 million tons). European plastic production accounted for 18.5% of total production in 2018, ranking third globally [2]. Waste plastic takes up a considerable proportion of municipal solid waste (MSW). Moreover, polypropylene (PP) accounts for nearly 24.3% of waste plastic, the highest percentage of plastic in MSW [3]. Many plastics are directly discarded due to improper disposal [4]. It is estimated that approximately 12,000 million tons of plastic will be landfilled or abandoned in the natural environment by 2050 [5]. Plastic leakage has caused severe damage to the environment [6]. Plastic debris presented in freshwater, marine, and soil environments has caused damage to these ecosystems [7], and further may pose a threat to human health [8]. Therefore, it is necessary to attach importance to and improve plastic recycling, particularly waste polypropylene (WPP).

Pyrolysis (thermal decomposition under an oxygen-free atmosphere [9–11]) is a widely used method for the chemical recycling of WPP to recover value-added products [12]. The pyrolysis products are oil, gas, and char [13–17]. The WPP pyrolysis oil is considered a potential substitute for commercial diesel [18–21]. Therefore, many works have been conducted to investigate the oil recovered from the pyrolysis of polypropylene (PP).

Temperature is one of the most critical parameters affecting PP pyrolysis oil yield [22]. Abbas-Abadi et al. [23] investigated PP pyrolysis at 420 °C to 510 °C. The oil yield was enhanced from 88.6 wt% at 420 °C to 92.3 wt% at 450 °C. In contrast, the oil yield was dramatically decreased to 76.1 wt% when the temperature ramped to 510 °C. Singh et al. [24, 25] studied WPP's thermal degradation on a broader temperature range, from 450 °C to 600 °C. The highest oil yield of 86.5 wt% was achieved at 500 °C. Achilias et al. [26] suggested that the PP and WPP pyrolysis oil yields were

✉ Gérald Debenest
gerald.debenest@toulouse-inp.fr

[1] Institut de Mécanique des Fluides de Toulouse (IMFT) - Université de Toulouse, CNRS-INPT-UPS, 31400 Toulouse, France

[2] Laboratory of Combustion and Combustible Matter (LCC), PPGEM, Federal University of Espírito Santo, Vitória 29075-910, Brazil

67.3 wt% and 64.7 wt% at 450 °C, respectively. A relatively lower oil yield of 56.9 wt% was gained at 500 °C by thermal decomposition of WPP [27].

Residence time (heating duration after reaching the desired temperature) and carrier gas are also significant parameters in the thermal degradation of polymers [3]. Lopez-Urionabarrenechea et al. [28] studied the impact of residence time on the pyrolysis of waste plastic. The oil yield significantly increased from 49.2 wt% (under 0 min) to 65.2 wt% (under 30 min) at 500 °C. While the oil yield slightly decreased by approximately 1.0 wt% when residence time ramped to 120 min. Residence time is a non-negligible parameter in the plastic pyrolysis process, peculiarly when the operating temperature is lower than 450 °C [3].

The types of carrier gas have remarkable impacts on oil yield [23]. PP pyrolysis oil production could be enhanced from 84.8 wt% in the argon atmosphere to 96.7 wt% in the hydrogen atmosphere. In comparison, the oil yield was merely 51.3 wt% in the absence of carrier gas. It is noteworthy that the oil yield was also up to 92.3 wt% by using nitrogen as the carrier gas. Therefore, nitrogen is recommended as the carrier gas during plastic pyrolysis due to its moderate price and handling safety [3]. Lin et al. [29, 30] also studied the impact of carrier gas flow rate (nitrogen) on the thermal decomposition of PP. They concluded that the carrier gas flow rate considerably affected the distribution of pyrolysis products. It is noteworthy that the aforementioned operating parameters are for the semi-batch reactor, which is widely used in bench-scale experiments due to its simplicity of operation and low cost.

In the above discussion, the impacts of different parameters on PP pyrolysis oil yield seems widely discussed. Subsequently, the operating parameters were optimized to obtain the maximum oil yield. However, legionary works were studied by varying operating parameters one-by-one [31–34]. Considering the operating parameters have complicated interactive effects on pyrolysis oil yield [35], the impacts of operating parameters on oil production were not described in-depth in these studies. The optimal operating parameters for oil yield determined by varying parameters one-by-one were also not particularly persuasive. Therefore, the present work comprehensively studies the impacts of operating parameters (carrier gas flow rate, residence time, and temperature) on WPP pyrolysis oil production and optimizes the parameters to achieve the highest oil yield. The neural fuzzy model coupled with a genetic algorithm has been proposed to achieve this goal. The impacts of operating parameters on WPP pyrolysis oil components are also investigated by FTIR and GC/MS analyses.

Fig. 1 WPP particles recycled from MSW

Table 1 The elemental analysis of WPP

Element	%
C	82.9 ± 0.1
H	10.2 ± 0.1
N	0.6 ± 0.0
S	0
Other elements[a]	6.3 ± 0.3

[a]Calculated by difference

Materials and methods

Materials

WPP was recycled from municipal solid waste (MSW) and made into ~ 3 mm granules (Fig. 1). It was received from Zhoushan Jinke Renewable Resources Co., Ltd., Zhejiang, China. Moreover, Table 1 lists the elemental analysis of WPP.

Pyrolysis experiment

The semi-batch reactor is favored for plastic pyrolysis due to its convenience of operation [3]. Thus, the WPP pyrolysis tests were carried out in a 200 mL lab-scale reactor. The initial weight of the WPP sample was ~ 5 g in each test. Nitrogen (under the flow rate of 100 mL/min) purged the reactor for 30 min to exhaust oxygen before the start of each test. The heating rate and pressure were maintained at 6 °C/min and 0.1 MPa, respectively. The detailed operating conditions of the WPP pyrolysis experiment are listed in Table 2. 17 sets of pyrolysis experiments (T1–T17) were conducted to obtain the training data. Also, five sets of pyrolysis experiments (V1–V5) were conducted to obtain the testing data. It should be stated that WPP could be

Table 2 Operating conditions of WPP pyrolysis experiment

Test	Temperature, °C	Residence time, min	Carrier gas flow rate, mL/min
T1	400	20	50
T2	400	20	150
T3	400	40	100
T4	400	60	50
T5	400	60	150
T6	450	20	50
T7	450	20	100
T8	450	40	50
T9	450	40	100
T10	450	40	150
T11	450	60	100
T12	450	60	150
T13	500	20	50
T14	500	20	150
T15	500	40	100
T16	500	60	50
T17	500	60	150
V1	425	30	125
V2	425	50	75
V3	475	30	125
V4	475	50	75
V5[a]	456	20	50

[a]Operating conditions optimized by neural fuzzy model coupled with genetic algorithm

completely pyrolyzed under all conditions. Each experiment was repeated twice to ensure the reproducibility of the experiment.

Characterization of oil

FTIR was used to identify the functional groups of WPP pyrolysis oil. GC/MS analyzed the chemical components of WPP pyrolysis oil based on National Institute of Standards and Technology (NIST) database of mass spectrum library. The operational details of FTIR and GC/MS are tabulated in Table 3.

The WPP pyrolysis oil is divided into three parts based on the carbon number: light (C8–C11), middle (C12–C20), and heavy (C21–C34) fractions, respectively.

$$Light\,fraction = \frac{\sum_{i=8}^{11} C_i(area\%)}{\sum_{i=8}^{34} C_i(area\%)} \times 100\% \quad (1)$$

$$Middle\,fraction = \frac{\sum_{i=12}^{20} C_i(area\%)}{\sum_{i=8}^{34} C_i(area\%)} \times 100\% \quad (2)$$

$$Heavy\,fraction = \frac{\sum_{i=21}^{34} C_i(area\%)}{\sum_{i=8}^{34} C_i(area\%)} \times 100\%, \quad (3)$$

where $C_i(area\%)$ represents each component's percentage.

Optimization method

The neural fuzzy model coupled with a genetic algorithm, illustrated in Fig. 2, was utilized to identify the optimal operating parameters for WPP pyrolysis oil production. The neural fuzzy model was described detail in Section A.1. It should be noted that the response surface methodology (RSM) is also widely used for data prediction. However, the RSM prediction accuracy is lower than the fuzzy neural model in some applications [35]. The model consisted of three parts: input layer, hidden layers, and output layer [37–39], respectively. The input layer had three parameters: carrier gas flow rate, residence time, and temperature. After the data training of the hidden layers, the output layer could determine the arithmetic expression between oil yield and operating parameters. Ulteriorly, a genetic algorithm was used to identify the optimal operating parameters for the highest WPP pyrolysis oil yield. Genetic algorithm has been detailed introduced in the previous study [40].

Table 3 Characterization experiment details of WPP pyrolysis oil

Name	Model	Operating conditions	References
FTIR	Thermo Nicolet 6700	Wavelength of 4000 cm^{-1} to 400 cm^{-1} with 4 cm^{-1} resolution	Xu et al. [36]
GC/MS	GC: Thermo Scientific TRACE 1300/1310 MS: Thermo Fisher TSQ 9000	GC front inlet temperature: 280 °C Mode of front inlet: Split Carrier gas: Helium under 1 mL/min Capillary column: 30 m × 0.25 mm, ID × 0.25 μm film GC temperature setting: Hold at 70 °C for 2 min; Ramp at 10 °C/min to 250 °C; Hold at 250 °C for 10 min; Ramp at 20 °C /min to 300 °C; Hold at 300 °C for 27.5 min MS transfer line temperature: 280 °C Temperature of ion source: 230 °C MS scan: 30 Da – 800 Da	National Institute of Standards and Technology (NIST) mass spectrum library

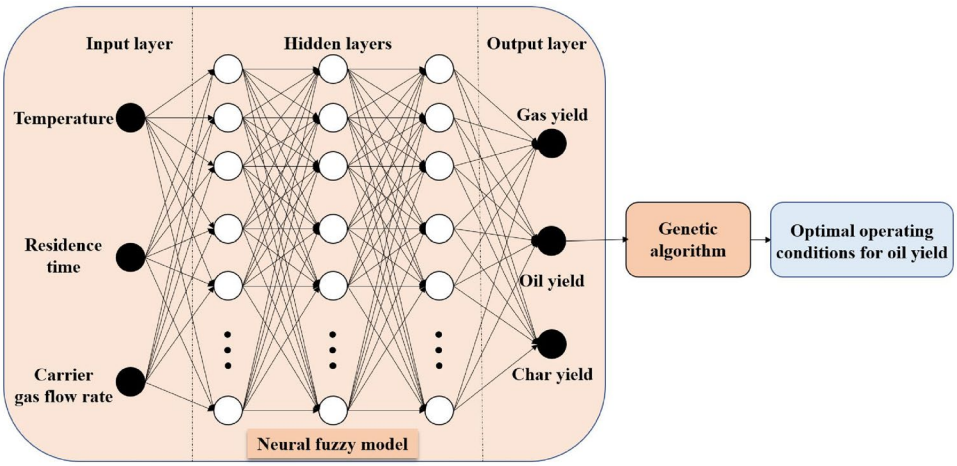

Fig. 2 The schematic representation of neural fuzzy model coupled with genetic algorithm

Results and discussion

Accuracy of neural fuzzy model

This study focuses on WPP thermal pyrolysis's oil yield. The WPP pyrolysis products were oil, gas, and char. It should be noted that the char refers to coke/semi-coke in this study, which contains heavy hydrocarbons that cannot flow out of the reactor [41]. From the perspective of getting a comprehensive understanding of the WPP pyrolysis process, the gas and char yields under different operating parameters were also investigated. Figure 3 demonstrates the experimental and neural fuzzy model predicted oil, gas, and char yields. Figure 3a, b show that the WPP pyrolysis oil yield varied from 59.8 wt% to 68.4 wt%. The results were very close to the values obtained by other researchers [17, 27, 42]. The pyrolysis of the virgin PP yields 88.6 wt% of oil at 420 °C [23], a value much higher than the WPP pyrolysis oil yield obtained in this study. This difference can be attributed to more tertiary carbons in recycled waste plastic compared to virgin plastic, which intensified the primary reactions [43]. Therefore, the WPP pyrolysis oil yield is lower than the value of virgin PP, and the WPP pyrolysis gas yield is higher than the value of virgin PP.

The WPP pyrolysis gas yield hovered from 12.6 wt% to 23.6 wt% (Fig. 3c, d), which was similar to the results in [17, 24, 42]. The char yield oscillated in a narrower range, from 15.5 wt% to 18.1 wt% (Fig. 3e, f). A char yield of 20.0 wt% was obtained by Achilias et al. [26], which was close to the values in this work.

Figure 3a, b suggests that the absolute relative errors of oil yield were lower than 0.5% and 1.6% in the training and testing sets, respectively. The absolute relative errors of gas and char yields were all within 6.0% (Fig. 3c–f). Moreover, the R-squared values and average absolute relative deviations (AARD) [44, 45] were 0.9998, 1.3%, and 0.9992, 2.3% for the neural fuzzy model's training and testing sets, respectively. It indicates that the neural fuzzy model predicted the yields of WPP pyrolysis products with a high degree of accuracy and reliability.

Interactions of residence time and carrier gas flow rate

Figure 4 depicts the interactions of residence time and carrier gas flow rate on WPP pyrolysis oil, gas, and char yields. It should be noted that the neural fuzzy model establishes the relationships of the pyrolysis product yields and operating conditions. Figure 4a illustrates that the oil yield decreased from 67.6 wt% (under 150 mL/min) to 63.0 wt% (under 50 mL/min) at 400 °C. While the gas yield increased from 12.3 wt% (under 50 mL/min) to 18.6 wt% (under 150 mL/min) at 400 °C (Fig. 4b). Some researchers ascribed the reduction of oil yield to insufficient condensation [46]. However, this interpretation might not precisely explain the same phenomenon observed in other studies [47–49], of which the higher gas yield was obtained under the increased carrier gas flow rate. The reduced oil yield and enhanced gas yield might be caused by the suppression of gas repolymerization and recondensation reactions under higher carrier gas flow rates [48, 49]. Figure 4c demonstrates the low sensitivity of char yield to changes in carrier gas flow rate under 20 min and 400 °C. As the carrier gas flow rate increased, the char yield reduced from 17.2 wt% to 16.9 wt% under 60 min and 400 °C. The reduction of char yield under the longer residence time could be ascribed to the facilitation of heavy hydrocarbons' gasification in char residue [50].

Figure 4d–i suggests that increasing the carrier gas flow rate reduced the oil and char yields and enhanced the gas yield at 450 °C and 500 °C. The carrier gas flow rate and residence time significantly impacted the oil and gas yields at higher temperatures. For example, the oil and gas yields oscillated in broader ranges of 62.5–68.2 wt%, 13.9–20.8 wt%, and 59.8–67.3 wt%, 15.9–23.6 wt% at 450 °C and

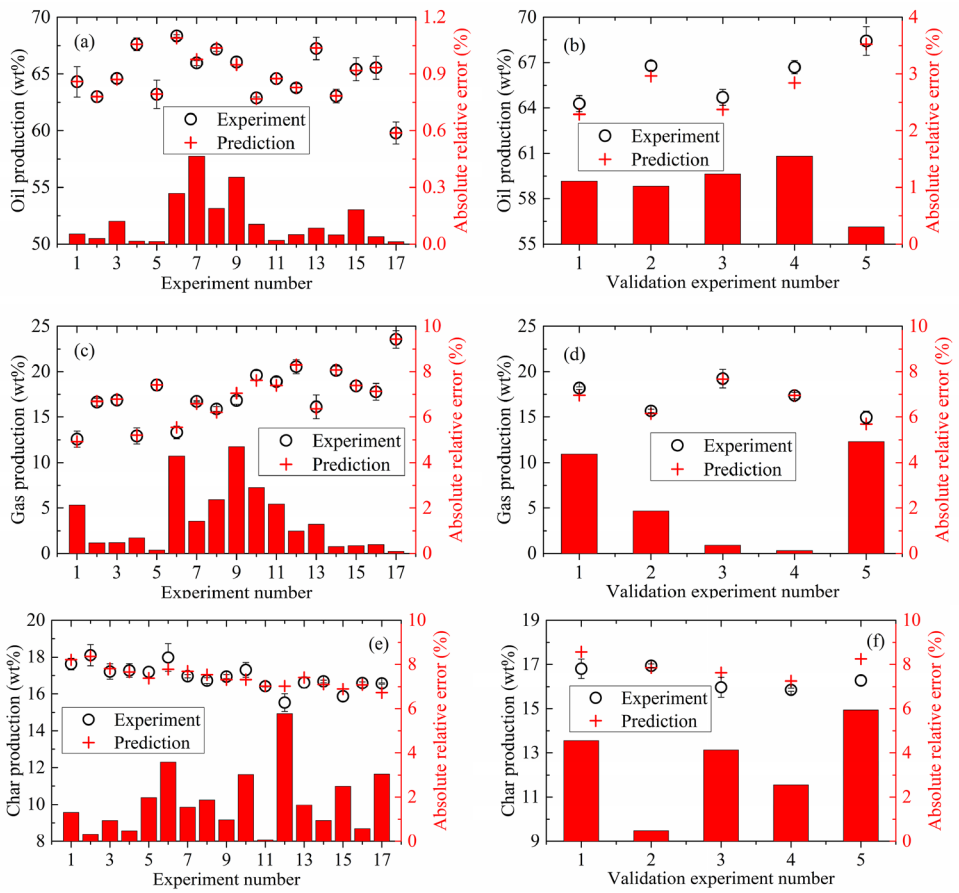

Fig. 3 Experimental oil, gas and char yields (black circle), neural fuzzy model predicted values (red cross), and absolute relative errors (red bar): **a** Oil yield in training set; **b** Oil yield in testing set; **c** Gas yield in training set; **d** Gas yield in testing set; **e** Char yield in training set; **f** Char yield in testing set

500 °C, respectively. Figure 4d demonstrates that the oil yield was higher at 450 °C compared to the ones at 400 °C and 500 °C. It is also noteworthy that the carrier gas flow rate became an inconsequential parameter on oil yield under the longer residence time at 450 °C. The oil yield slightly decreased by 1.2 wt% when the carrier gas flow rate increased at 450 °C and 60 min. While the carrier gas flow rate had a similar extent of increase in gas yield under different residence times at 400 °C, 450 °C, and 500 °C, respectively.

Interactions of carrier gas flow rate and temperature

Figure 5a, d demonstrates that the carrier gas flow rate and the temperature had similar interactive effects on oil yield under 20 min and 40 min. It could be observed that the oil yield increased with the temperature (400–450 °C) under lower carrier gas flow rates. Simultaneously, higher temperatures were not conducive to oil production at 450–500 °C. Higher temperatures could accelerate the WPP pyrolysis rate and generate more volatiles per unit time [51–53], resulting in a shorter residence time of the volatiles in the main reaction zone. The shortened residence time would suppress the oil from being decomposed into gas. Therefore, the increased temperature (400–450 °C) enhanced the oil yield from 64.4 wt% to 68.2 wt% under 20 min, and from 65.2 wt% to 67.3 wt% under 40 min. However, the oil yields were reduced to 67.3 wt% under 20 min and 66.8 wt% under 20 min at 500 °C, respectively. The decrease in oil yield was caused by the intense secondary cracking reactions for gas formation when the temperature increased from 450 °C to 500 °C [54].

Moreover, the temperature became a trivial factor on oil yield under higher carrier gas flow rates. For instance, the oil production varied in narrower ranges of 62.5–63.1 wt% (under 20 min) and 62.2–63.1 wt% (under 40 min) under 150 mL/min. As demonstrated in Fig. 5g (under 60 min), the oil yield decreased from 67.6 wt% (at 400 °C) to 59.8 wt% (at 500 °C). The increased temperature intensified the secondary cracking reactions of oil that reduced oil yield [55].

Higher temperatures enhanced the gas yield while suppressing the char yield regardless of the carrier gas flow rate and residence time changes (Figs. 5b–i). As the temperature increased, the gas yields increased from 12.3 wt% to 20.2 wt% (under 20 min), 15.1 wt% to 20.2 wt% (under 40 min), and 13.0 wt% to 23.6 wt% (under 60 min). Contrarily, the char yields decreased from 18.0 wt% to 16.5 wt%, 17.5 wt% to 16.3 wt%, and 17.2 wt% to 16.1 wt% at 400–500 °C,

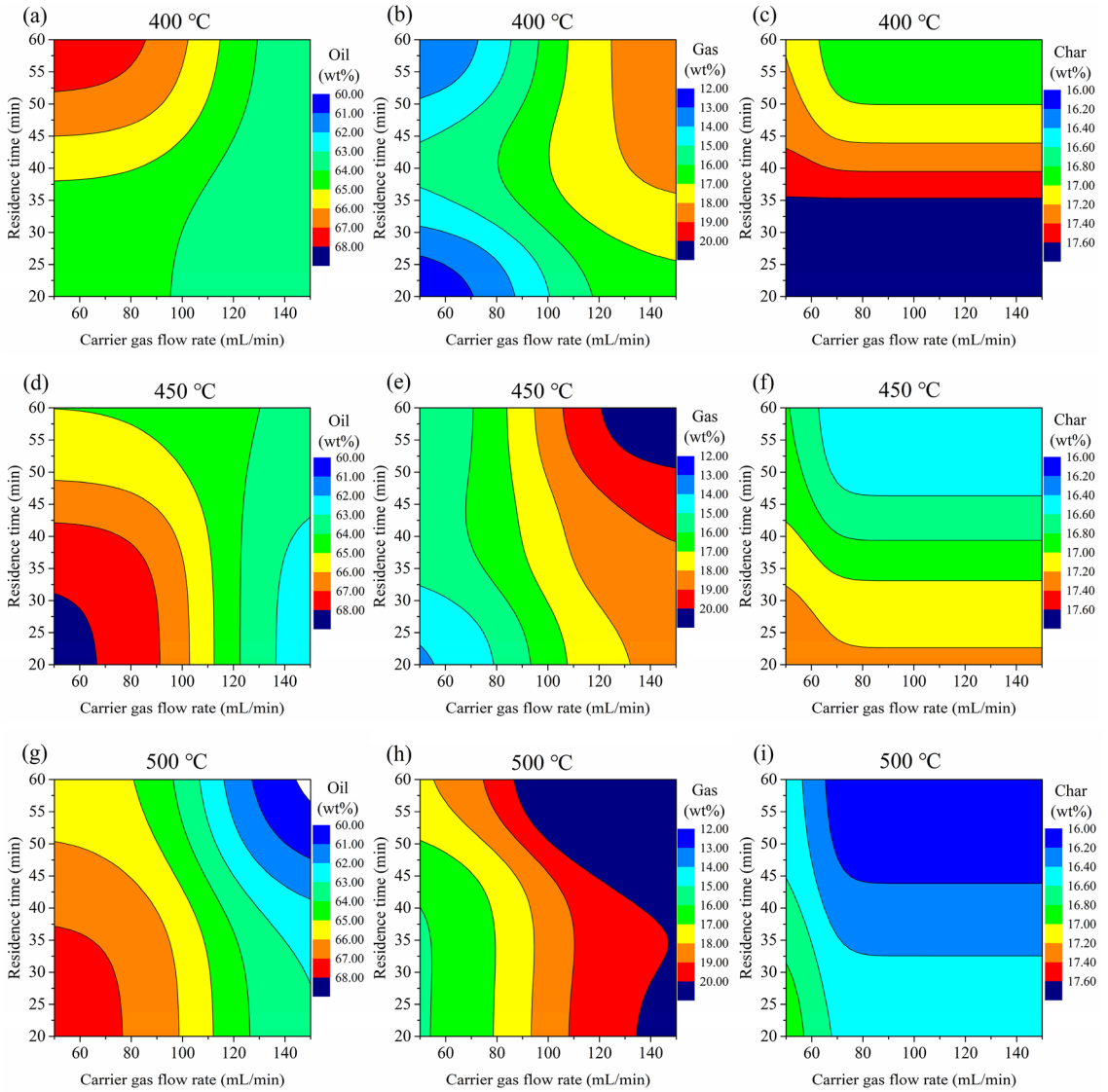

Fig. 4 Interactions of residence time and carrier gas flow rate on WPP pyrolysis oil, gas and char yields at different temperatures: **a** Oil yield at 400 ℃; **b** Gas yield at 400 ℃; **c** Char yield at 400 ℃; **d** Oil yield at 450 ℃; **e** Gas yield at 450 ℃; **f** Char yield at 450 ℃; **g** Oil yield at 500 ℃; **h** Gas yield at 500 ℃; **i** Char yield at 500 ℃

respectively. The decrease in char yield at higher temperatures could be ascribed to the gasification reactions that consumed hydrocarbons in char residues [56]. The enhanced gas yield might be caused by the intensified oil's secondary cracking and the char's gasification at higher temperatures, which were favorable to the gas yield [49].

Interactions of residence time and temperature

The oil yield increased at lower temperatures while decreasing at higher temperatures as the residence time extended. As the residence time extended, the oil production enhanced by 3.3 wt% under 50 mL/min (Fig. 6a), 2.3 wt% under 100 mL/min (Fig. 6d), and 0.2 wt% under 150 mL/min (Fig. 6g) at 400 °C, respectively. However, the oil yield reduced by 1.7 wt% (67.3–65.6 wt%) under 50 mL/min, 2.2 wt% (65.9–63.7 wt%) under 100 mL/min, and 3.3 wt% (63.1–59.8 wt%) under 150 mL/min at 500 °C, respectively. As the residence time extended from 20 to 40 min at the lowest temperature (400 °C), the gas yields enhanced by 2.9 wt% under 50 mL/min (Fig. 6b) and 2.0 wt% under 100 mL/min (Fig. 6e), respectively. The enhanced gas yield could be ascribed to the secondary cracking of long-chain hydrocarbons (wax) into short-chain hydrocarbons (heavy fraction's oil and gas). The wax cannot be carried out from the reactor at lower carrier gas flow rates. Consequently, the increase in oil production at lower temperatures might be caused by the wax decomposition under longer residence times. As

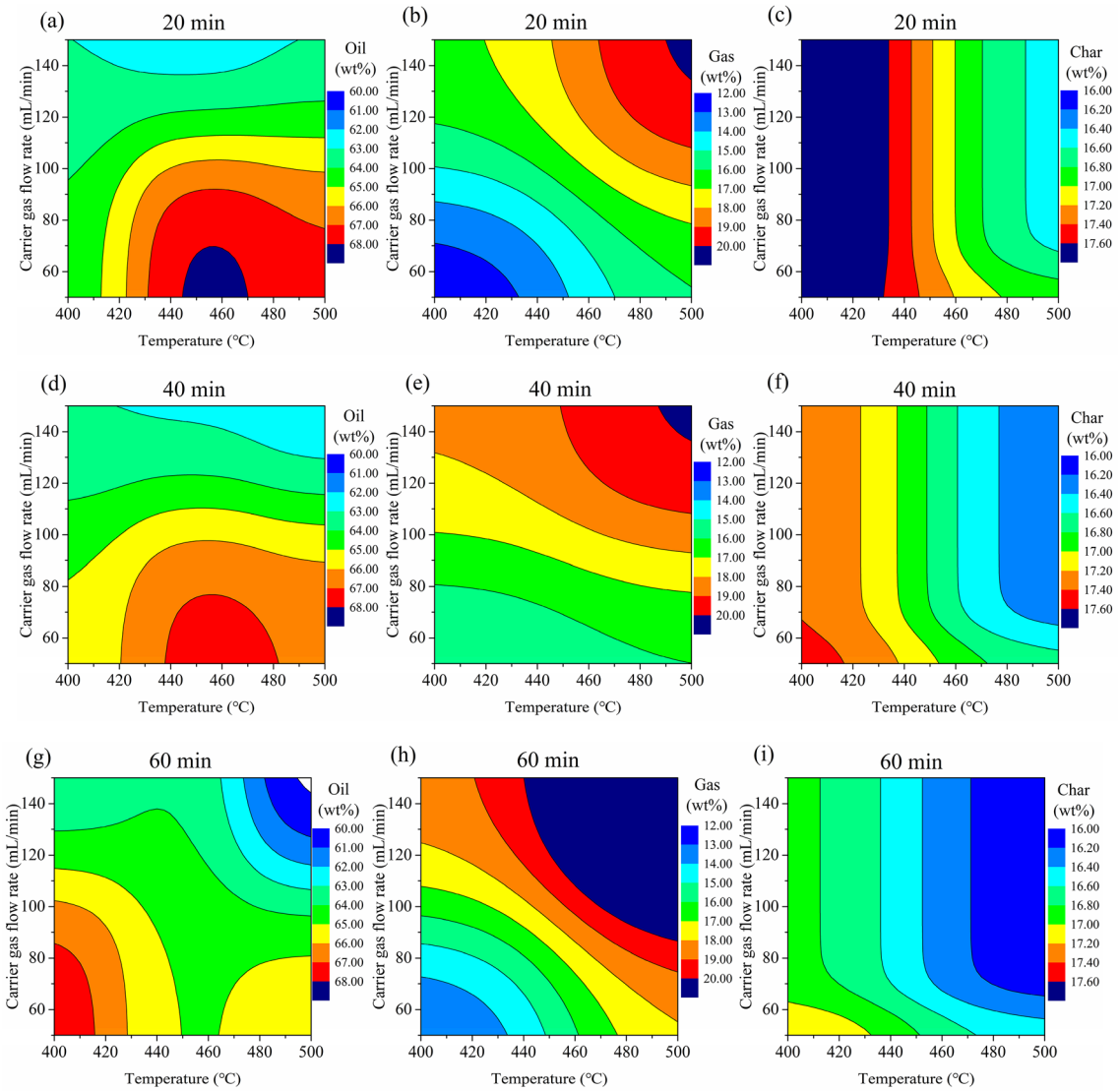

Fig. 5 Interactions of carrier gas flow rate and temperature on WPP pyrolysis oil, gas and char yields: **a** Oil yield under 20 min; **b** Gas yield under 20 min; **c** Char yield under 20 min; **d** Oil yield under 40 min; **e** Gas yield under 40 min; **f** Char yield under 40 min; **g** Oil yield under 60 min; **h** Gas yield under 60 min; **i** Char yield under 60 min

the residence time extended, the reduction in oil production at higher temperatures was caused by oil's more intensive secondary cracking reactions [57, 58].

As the residence time extended from 20 to 60 min under 150 mL/min, the gas yield enhanced from 16.7 wt% to 23.6 wt% (Fig. 6h), and the char yield decreased from 18.0 wt% to 16.1 wt% (Fig. 6i). Prolonged residence time deepened the oil secondary cracking and char gasification reactions, which elevated the gas yield. As depicted in Fig. 6c, f, and i, it could be distinctly observed that the highest char yields were all obtained at the lowest temperature (400 °C) and the shortest residence time (20 min). Moreover, the highest char yield increased from 17.9 wt% under 50 mL/min to 18.0 wt% under 100 mL/min. The enhanced char yield might be attributed to the worse efficiency of heat transfer in the reaction zone under higher carrier gas flow rates [49].

Genetic algorithm optimized operating parameters for oil yield

Figure 7 demonstrates the genetic algorithm optimization process and the optimized operating conditions for WPP pyrolysis oil yield. The optimized function was oil yield with the arguments of carrier gas flow rate, residence time, and temperature. As shown in Fig. 7a, the first iteration's average and optimal oil yields were 65.7 wt% and 66.1 wt%, respectively. The optimal and average values were stabilized at

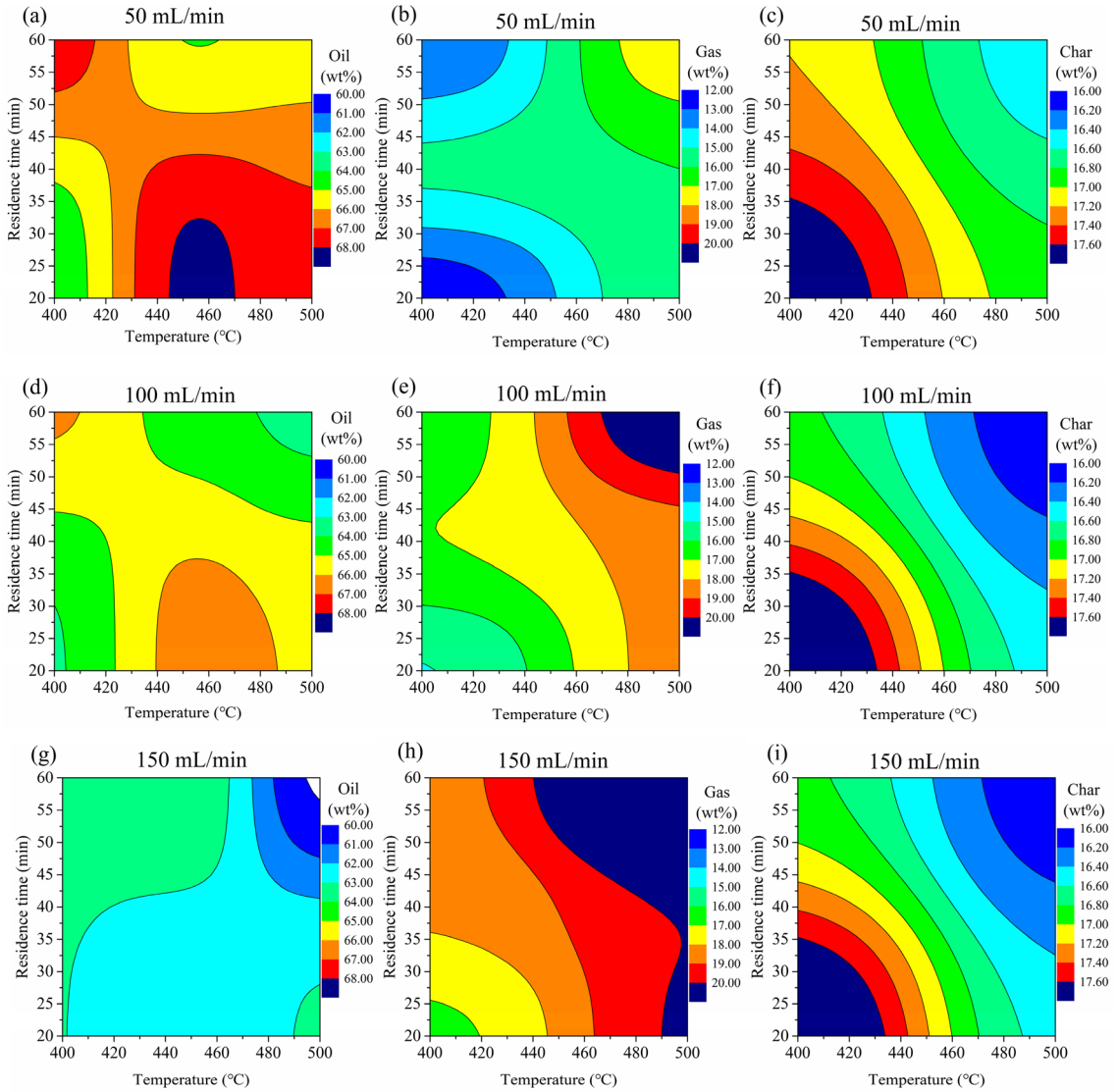

Fig. 6 Interactions of residence time and temperature on WPP pyrolysis oil, gas and char yields under different carrier gas flow rates: **a** Oil yield under 50 mL/min; **b** Gas yield under 50 mL/min; **c** Char yield under 50 mL/min; **d** Oil yield under 100 mL/min; **e** Gas yield under 100 mL/min; **f** Char yield under 100 mL/min; **g** Oil yield under 150 mL/min; **h** Gas yield under 150 mL/min; **i** Char yield under 150 mL/min

68.2 wt% after 87 and 856 iterations. It verified the superior astringency of the genetic algorithm.

As depicted in Fig. 7b, the oil yield optimized by the neural fuzzy model coupled with a genetic algorithm was 68.2 wt% under 456 °C, 20 min, and 50 mL/min. Experiment V5 in the training set was conducted under the optimized operating parameters to validate the accuracy of the genetic algorithm's predicted optimal value. The experimental oil yield under the optimized operating parameters was 68.4 wt%. The absolute relative error was merely 0.3% between the experimental and genetic algorithm optimized oil yields, which revealed the high reliability of the genetic algorithm. Consequently, it can conclude that the optimal operating parameters for WPP thermal pyrolysis oil production were 456 °C, 20 min, 50 mL/min.

FTIR analysis of oil

Figure A.3 shows the FTIR analysis of WPP pyrolysis oil samples in the training and testing sets. It could be distinctly observed that the locations and intensities of characteristic peaks did not change with the operating parameters. Table A.3 tabulates the main functional groups of WPP pyrolysis oil under the optimal operating parameters (456 °C, 20 min, and 50 mL/min). The following functional groups have been detected: $=C-H$ stretching at 3075 cm^{-1}, $-CH_2-$ stretching

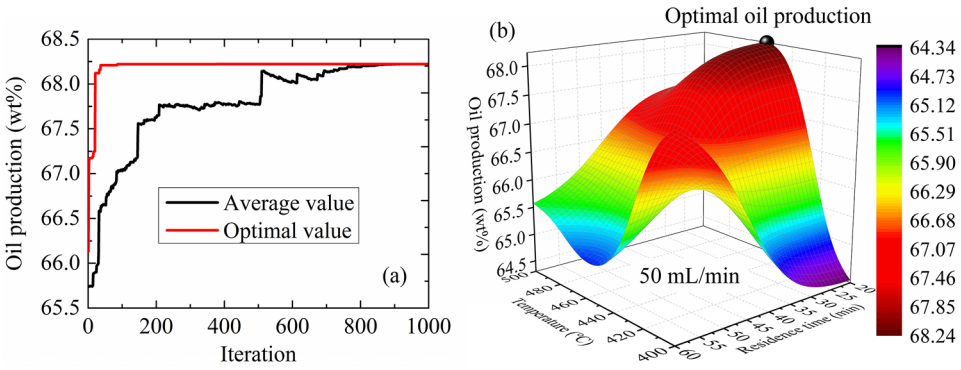

Fig. 7 Genetic algorithm optimized operating parameters for oil yield: **a** process of optimization; **b** optimal oil yield

at 2955 – 2846 cm^{-1}, – C = C – stretching at 1650 cm^{-1}, – CH_2 – scissoring at 1457 cm^{-1}, – CH_3 bending at 1377 cm^{-1}, – C = C – bending at 994 and 909 cm^{-1}, – C = CH_2 wagging at 971 cm^{-1}, and – CH_2 – rocking at 724 cm^{-1}. The oil compounds were mainly alkenes and alkanes, which corresponded with other research results [59–62].

The random scission reactions in the incipient stage of WPP decomposition were also known as the intermolecular hydrogen transfer reactions that responsibly generated the alkanes [25]. While the formation of the alkenes primarily corresponded to the summation of secondary cracking (Beta scission), disproportionation, and intramolecular hydrogen transfer reactions, which took place in the stage of termination [60].

GC/MS analysis of oil

Figure A.4 shows the GC/MS chromatogram of WPP pyrolysis oil under the optimal operating parameters (456 °C, 20 min, and 50 mL/min). The specific components in WPP pyrolysis oil under the optimized operating parameters are listed in Table A.4. It should be noted that there are limitations in analyzing the content of oil components because of the complex components of plastic pyrolysis oils [27, 28, 56]. Heavy components with a distillation point above 300 °C in oil samples cannot be detected by GC due to the GC temperature setting (Table 3). The WPP pyrolysis oil was composed of alkenes, alkanes, and naphthenes in C8–C34. The highest proportion in the oil was 2,4-dimethyl-1-heptene, which accounted for 11.9 area%, followed by 7.8 area% 1-pentadecene and 6.6 area% pentadecane. The high alkenes' yield was principally attributed to the oil's secondary cracking during the thermal pyrolysis of WPP [25].

Figure A.5 demonstrates the GC/MS chromatograms of WPP pyrolysis oil samples of T1–T17, respectively. The types of identified compounds presented in WPP pyrolysis oil samples were similar under different operating parameters. The oil samples were all composed of alkenes, alkanes, and naphthenes ranging from C8 to C34. In comparison, the proportions of each compound varied with the operating parameters. The oil was divided into three fractions based on the carbon number: light (C8–C11), middle (C12–C20), and heavy (C21–C34) fractions, respectively. Figure 8 depicts the fractions of WPP pyrolysis oil under different operating parameters. The most significant proportion of WPP pyrolysis oil was the middle fraction (40.1–44.0%), followed by the heavy (33.7–39.6%) and the light (19.9–23.9%) fractions.

Figure 9a illustrates that the temperature significantly impacted the distribution of oil fractions in samples T1, T6, and T13. As the temperature increased, the light fraction reduced from 23.9% to 21.5%, and the heavy fraction increased from 33.7 to 36.4%. The middle fraction increased from 42.4% to 44.0% when the temperature ramped from 400 °C to 450 °C and then reduced to 42.1% at 500 °C. Higher temperatures promoted the secondary cracking reactions of light fraction for pyrolysis gas formation, which simultaneously reduced the light fraction in oil [63, 64]. It could be concluded that low temperature was beneficial to the oil's light fraction formation.

Figure 9b depicts the influence of residence time on the distributions of WPP pyrolysis oil fractions (T7, T9, and T11). The extension of residence time increased in the middle and heavy fractions and decreased light

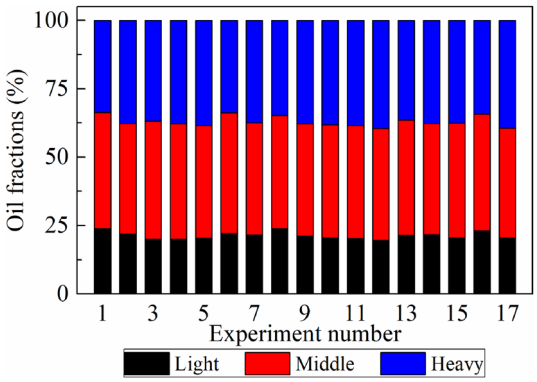

Fig. 8 Fractions of WPP pyrolysis oil under different operating parameters

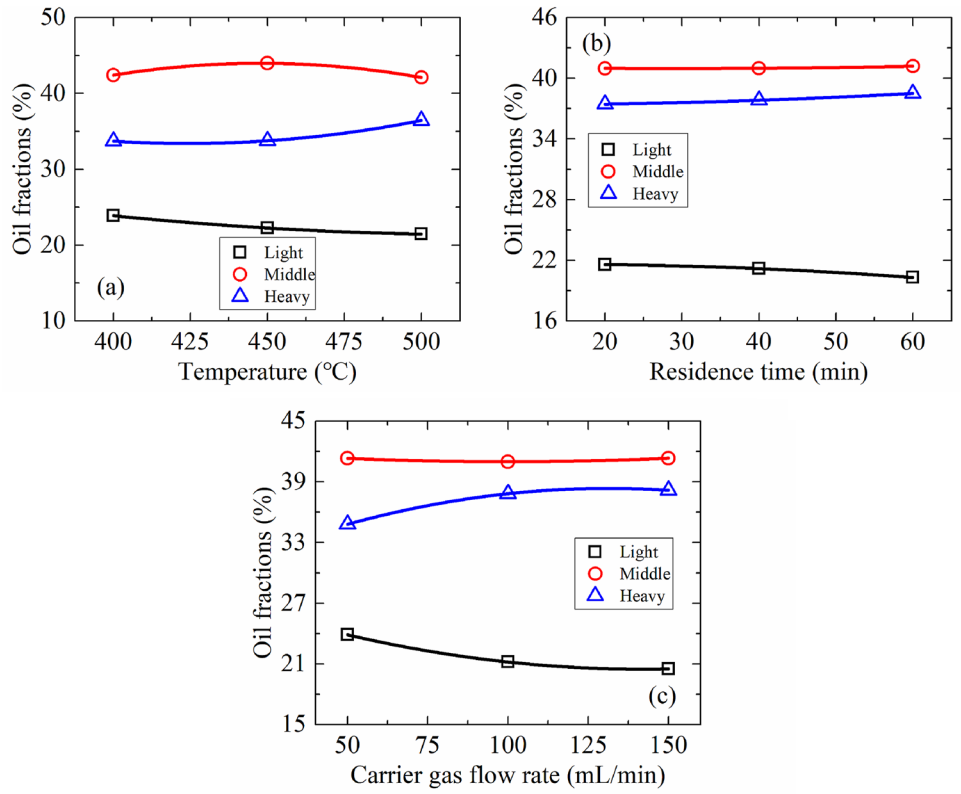

Fig. 9 Impacts of operating parameters on WPP pyrolysis oil fractions: **a** temperature; **b** residence time; **c** carrier gas flow rate

fraction [65]. The middle and heavy fractions increased by 0.2% and 1.1%, while the light fraction reduced by 1.3% as the residence time extended within the studied range. The decrease in the light fraction might be ascribed to the greater probability of secondary cracking reactions under longer residence time. In this perspective, shorter residence time was conducive to producing lighter WPP pyrolysis oil.

Figure 9c demonstrates the impact of carrier gas flow rate on the distribution of WPP pyrolysis oil fractions (T8, T9, and T10). The light fraction reduced from 23.9% to 20.5% when the carrier gas flow rate ramped from 50 mL/min to 150 mL/min, while the heavy fraction increased from 34.8% to 38.2%. The middle fraction reduced from 41.3% to 41.0% when the carrier gas flow rate increased from 50 mL/min to 100 mL/min and then enhanced to 41.3% under 150 mL/min. The non-condensable pyrolysis gas was quickly removed from the main reaction region under the higher flow rate of carrier gas, which subsequently suppressed the repolymerization and recondensation reactions for the formation of light fraction in oil [66, 67]. The increase in the heavy fraction was caused by the inhibition of secondary cracking reactions as the flow rate of carrier gas increased, resulting in a reduction of light fraction in oil.

Conclusions

This study comprehensively studied the interactions of operating parameters (carrier gas flow rate, residence time, and temperature) on the distribution of waste polypropylene (WPP) pyrolysis products. The objective was to maximize the WPP pyrolysis oil yield by regulating the operating parameters. The gas and char yields were also investigated to comprehensively understand the WPP thermal pyrolysis process. It is noteworthy that the test of a diesel engine fueled with the WPP pyrolysis oil will be conducted in future work.

A hybrid neural fuzzy network model coupled with a genetic algorithm was used to optimize the operating parameters for WPP pyrolysis oil yield. It should be noted that this method can be applied to practical applications with more complex operating conditions. The highest oil yield of 68.4 wt% was achieved under 456 °C, 20 min, and 50 mL/min. The oil was composed of alkenes, alkanes, and naphthenes in C8–C34. The highest proportion in the oil was 2,4-dimethyl-1-heptene, which accounted for 11.9%, followed by 7.8% 1-pentadecene and 6.6% pentadecane.

The types of main functional groups of the WPP pyrolysis oil did not change with the operating parameters.

Lower temperature, shorter residence time, and lower carrier gas flow rate were conducive to forming oil's light fraction. While higher temperature, longer residence time, and higher carrier gas flow rate resulted in a high oil's heavy fraction production.

Supplementary Information The online version contains supplementary material available at https://doi.org/10.1007/s10163-022-01521-7.

Acknowledgements This work was supported by the China Scholarship Council (CSC) program (No. 201906120036). Thanks are given to Dr. Yue ZAN from LCC-CNRS-UPS (Laboratoire de Chimie de Coordination du CNRS, Université Toulouse III—Paul Sabatier) for her assistance in the FTIR test and analysis.

Declarations

Conflict of interest The authors declare that they have no known competing financial interests or personal relationships that could have appeared to influence the work reported in this paper.

References

1. Van Eygen E, Feketitsch J, Laner D, Rechberger H, Fellner J (2017) Comprehensive analysis and quantification of national plastic flows: the case of Austria. Resour Conserv Recy 117:183–194. https://doi.org/10.1016/j.resconrec.2016.10.017
2. Leal Filho W, Salvia AL, Bonoli A, Saari UA, Voronova V, Kloga M, Kumbhar SS, Olszewski K, De Quevedo DM, Barbir J (2021) An assessment of attitudes towards plastics and bioplastics in Europe. Sci Total Environ 755(1):142732. https://doi.org/10.1016/j.scitotenv.2020.142732
3. Sharuddin SDA, Abnisa F, Daud WMAW, Aroua MK (2016) A review on pyrolysis of plastic wastes. Energy Convers Manag 115:308–326. https://doi.org/10.1016/j.enconman.2016.02.037
4. Chae Y, An YJ (2018) Current research trends on plastic pollution and ecological impacts on the soil ecosystem: a review. Environ Pollut 240:387–395. https://doi.org/10.1016/j.envpol.2018.05.008
5. Geyer R, Jambeck JR, Law KL (2017) Production, use, and fate of all plastics ever made. Sci Adv 3(7):e1700782. https://doi.org/10.1126/sciadv.1700782
6. Al-harahsheh M, Al-Nuairat J, Al-Otoom A, Al-hammouri I, Al-jabali H, Al-zoubi M, Abu Alasal S (2019) Treatments of electric arc furnace dust and halogenated plastic wastes: a review. J Environ Chem Eng 7(1):102856. https://doi.org/10.1016/j.jece.2018.102856
7. Blettler MCM, Abrial E, Khan FR, Sivri N, Espinola LA (2018) Freshwater plastic pollution: recognizing research biases and identifying knowledge gaps. Water Res 143:416–424. https://doi.org/10.1016/j.watres.2018.06.015
8. Bouwmeester H, Hollman PCH, Peters RJB (2015) Potential health impact of environmentally released micro- and nanoplastics in the human food production chain: experiences from nanotoxicology. Environ Sci Technol 49(15):8932–8947. https://doi.org/10.1021/acs.est.5b01090
9. Al-Salem SM, Antelava A, Constantinou A, Manos G, Dutta A (2017) A review on thermal and catalytic pyrolysis of plastic solid waste (PSW). J Environ Manag 197:177–198. https://doi.org/10.1016/j.jenvman.2017.03.084
10. Pan R, Debenest G (2022) Numerical investigation of a novel smoldering-driven reactor for plastic waste pyrolysis. Energy Convers Manag 257:115439. https://doi.org/10.1016/j.enconman.2022.115439
11. Huang J, Veksha A, Chan WP, Giannis A, Lisak G (2022) Chemical recycling of plastic waste for sustainable material management: a prospective review on catalysts and processes. Renew Sustain Energy Rev 154:111866. https://doi.org/10.1016/j.rser.2021.111866
12. Lopez G, Artetxe M, Amutio M, Bilbao J, Olazar M (2017) Thermochemical routes for the valorization of waste polyolefinic plastics to produce fuels and chemicals. A review. Renew Sustain Energy Rev 73:346–368. https://doi.org/10.1016/j.rser.2017.01.142
13. Singh TK, Rajak U, Dasore A, Muthukumar M, Verma TN (2021) Performance and ecological parameters of a diesel engine fueled with diesel and plastic pyrolyzed oil (PPO) at variable working parameters. Environ Technol Innov 22:101491. https://doi.org/10.1016/j.eti.2021.101491
14. Qureshi MS, Oasmaa A, Pihkola H, Deviatkin I, Tenhunen A, Mannila J, Minkkinen H, Pohjakallio M, Laine-Ylijoki J (2020) Pyrolysis of plastic waste: opportunities and challenges. J Anal Appl Pyrol 152:104804. https://doi.org/10.1016/j.jaap.2020.104804
15. Antelava A, Jablonska N, Constantinou A, Manos G, Salaudeen SA, Dutta A, Al-Salem SM (2021) Energy potential of plastic waste valorization: a short comparative assessment of pyrolysis versus gasification. Energy Fuels 35(5):3558–3571. https://doi.org/10.1021/acs.energyfuels.0c04017
16. Chen X, Wang Y, Zhang L (2021) Recent progress in the chemical upcycling of plastic wastes. Chemsuschem 14(19):4137–4151. https://doi.org/10.1002/cssc.202100868
17. Sogancioglu M, Yel E, Ahmetli G (2020) Behaviour of waste polypropylene pyrolysis char-based epoxy composite materials. Environ Sci Pollut Res 27:3871–3884. https://doi.org/10.1007/s11356-019-07028-3
18. Soni VK, Singh G, Vijayan BK, Chopra A, Kapur GS, Ramakumar SSV (2021) Thermochemical recycling of waste plastics by pyrolysis: a review. Energy Fuels 35(16):12763–12808. https://doi.org/10.1021/acs.energyfuels.1c01292
19. Mani M, Subash C, Nagarajan G (2009) Performance, emission and combustion characteristics of a DI diesel engine using waste plastic oil. Appl Therm Eng 29:2738–2744. https://doi.org/10.1016/j.applthermaleng.2009.01.007
20. Kalargaris I, Tian G, Gu S (2017) The utilisation of oils produced from waste plastic at different pyrolysis temperatures in a DI diesel engine. Energy 131:179–185. https://doi.org/10.1016/j.energy.2017.05.024
21. Mangesh VL, Padmanabhan S, Tamizhdurai P, Narayanan S, Ramesh A (2020) Combustion and emission analysis of hydrogenated waste polypropylene pyrolysis oil blended with diesel. J Hazard Mater 386:121453. https://doi.org/10.1016/j.jhazmat.2019.121453
22. Zhang F, Zhao YT, Wang DD, Yan MQ, Zhang J, Zhang PY, Ding TG, Chen L, Chen C (2021) Current technologies for plastic waste treatment: a review. J Clean Prod 282:124523. https://doi.org/10.1016/j.jclepro.2020.124523
23. Abbas-Abadi MS, Haghighi MN, Yeganeh H, McDonald AG (2014) Evaluation of pyrolysis process parameters on polypropylene degradation products. J Anal Appl Pyrol 109:272–277. https://doi.org/10.1016/j.jaap.2014.05.023
24. Singh RK, Ruj B, Sadhukhan AK, Gupta P (2019) Thermal degradation of waste plastics under non-sweeping atmosphere: part 1: effect of temperature, product optimization, and degradation mechanism. J Environ Manage 239:395–406. https://doi.org/10.1016/j.jenvman.2019.03.067
25. Singh RK, Ruj B, Sadhukhan AK, Gupta P (2020) Thermal degradation of waste plastics under non-sweeping atmosphere: part 2:

effect of process temperature on product characteristics and their future applications. J Environ Manag 261:110112. https://doi.org/10.1016/j.jenvman.2020.110112
26. Achilias DS, Roupakias C, Megalokonomos P, Lappas AA, Antonakou EV (2007) Chemical recycling of plastic wastes made from polyethylene (LDPE and HDPE) and polypropylene (PP). J Hazard Mater 149(3):536–542. https://doi.org/10.1016/j.jhazmat.2007.06.076
27. Quesada L, Calero M, Martin-Lara MA, Perez A, Blazquez G (2020) Production of an alternative fuel by pyrolysis of plastic wastes mixtures. Energ Fuel 34(2):1781–1790. https://doi.org/10.1021/acs.energyfuels.9b03350
28. Lopez-Urionabarrenechea A, de Marco I, Caballero BM, Laresgoiti MF, Adrados A (2011) Influence of time and temperature on pyrolysis of plastic wastes in a semi-batch reactor. Chem Eng J 173(1):62–71. https://doi.org/10.1016/j.cej.2011.07.037
29. Lin YH, Yen HY (2005) Fluidised bed pyrolysis of polypropylene over cracking catalysts for producing hydrocarbons. Polym Degrad Stab 89(1):101–108. https://doi.org/10.1016/j.polymdegradstab.2005.01.006
30. Lin YH, Yang MH (2007) Catalytic pyrolysis of polyolefin waste into valuable hydrocarbons over reused catalyst from refinery FCC units. Appl Catal A-Gen 328(2):132–139. https://doi.org/10.1016/j.apcata.2007.05.039
31. Matamba T, Tahmasebi A, Rish SK, Yu JL (2021) Understanding the enhanced production of poly-aromatic hydrocarbons during the pyrolysis of lignocellulosic biomass components under pressurized entrained-flow conditions. Fuel Process Technol 213:106645. https://doi.org/10.1016/j.fuproc.2020.106645
32. Zaini IN, Wen YM, Mousa E, Jonsson PG, Yang WH (2021) Primary fragmentation behavior of refuse derived fuel pellets during rapid pyrolysis. Fuel Process Technol 216:106796. https://doi.org/10.1016/j.fuproc.2021.106796
33. Zhang JL, Wang L, Ni HX, Shi QP, Zhang XY, Yu HB, Ma FY (2021) Selective fungal pretreatment favored pyrolysis products of wheat straw based on pyrolytic polygeneration system. Fuel Process Technol 215:106749. https://doi.org/10.1016/j.fuproc.2021.106749
34. del Pozo C, Rego F, Puy N, Bartroli J, Fabregas E, Bridgwater AV (2021) Converting coffee silverskin to value-added products by a slow pyrolysis-based biorefinery process. Fuel Process Technol 214:106708. https://doi.org/10.1016/j.fuproc.2020.106708
35. Quesada L, Perez A, Godoy V, Peula FJ, Calero M, Blazquez G (2019) Optimization of the pyrolysis process of a plastic waste to obtain a liquid fuel using different mathematical models. Energy Convers Manag 188:19–26. https://doi.org/10.1016/j.enconman.2019.03.054
36. Xu FF, Wang B, Yang D, Hao JH, Qiao YY, Tian YY (2018) Thermal degradation of typical plastics under high heating rate conditions by TG-FTIR: pyrolysis behaviors and kinetic analysis. Energy Convers Manag 171:1106–1115. https://doi.org/10.1016/j.enconman.2018.06.047
37. Prabhakaran SPS, Swaminathan G, Joshi VV (2020) Energy conservation – a novel approach of co-combustion of paint sludge and Australian lignite by principal component analysis, response surface methodology and artificial neural network modeling. Environ Technol Innov 20:101061. https://doi.org/10.1016/j.eti.2020.101061
38. Altowayti WAH, Haris SA, Almoalemi H, Shahir S, Zakaria Z, Ibrahim S (2020) The removal of arsenic species from aqueous solution by indigenous microbes: batch bioadsorption and artificial neural network model. Environ Technol Innov 19:100830. https://doi.org/10.1016/j.eti.2020.100830
39. Kassahun SK, Kiflie Z, Kim H, Baye AF (2021) Process optimization and kinetics analysis for photocatalytic degradation of emerging contaminant using N-doped TiO2-SiO2 nanoparticle: artificial neural network and surface response methodology approach. Environ Technol Innov 23:101761. https://doi.org/10.1016/j.eti.2021.101761
40. Pan R, Duque JVF, Debenest G (2021) Investigating waste plastic pyrolysis kinetic parameters by genetic algorithm coupled with thermogravimetric analysis. Waste Biomass Valor 12:2623–2637. https://doi.org/10.1007/s12649-020-01181-4
41. Qian M, Lei H, Zhao Y, Villota E, Huo E, Wang C, Zhang X (2021) Lignin-mediated preparation of hierarchical ZSM-5 catalysts and their effects in the catalytic co-pyrolysis of softwood biomass and low-density polyethylene mixtures. ACS Sustain Chem Eng 9(37):12602–12613. https://doi.org/10.1021/acssuschemeng.1c03863
42. Lubongo C, Congdon T, McWhinnie J, Alexandridis P (2022) Economic feasibility of plastic waste conversion to fuel using pyrolysis. Sustain Chem Pharm 27:100683. https://doi.org/10.1016/j.scp.2022.100683
43. Abbas-Abadi MS, Zayoud A, Kusenberg M et al (2022) Thermochemical recycling of end-of-life and virgin HDPE: a pilot-scale study. J Anal Appl Pyrolysis. https://doi.org/10.1016/j.jaap.2022.105614
44. Wang K, Xu HJ, Yang C, Qiu T (2020) Machine learning-based ionic liquids design and process simulation for CO2 separation from flue gas. Green Energy Environ. https://doi.org/10.1016/j.gee.2020.12.019
45. Shi HW, Zhang X, Sundmacher K, Zhou T (2020) Model-based optimal design of phase change ionic liquids for efficient thermal energy storage. Green Energy Environ. https://doi.org/10.1016/j.gee.2020.12.017
46. Varma AK, Mondal P (2017) Pyrolysis of sugarcane bagasse in semi batch reactor: effects of process parameters on product yields and characterization of products. Ind Crops Prod 95:704–717. https://doi.org/10.1016/j.indcrop.2016.11.039
47. Morali U, Sensoz S (2015) Pyrolysis of hornbeam shell (Carpinus betulus L.) in a fixed bed reactor: characterization of bio-oil and bio-char. Fuel 150:672–678. https://doi.org/10.1016/j.fuel.2015.02.095
48. Saikia R, Chutia RS, Kataki R, Pant KK (2015) Perennial grass (Arundo donax L.) as a feedstock for thermo-chemical conversion to energy and materials. Bioresour Technol 188:265–272. https://doi.org/10.1016/j.biortech.2015.01.089
49. Xu FF, Ming X, Jia R, Zhao M, Wang B, Qiao YY, Tian YY (2020) Effects of operating parameters on products yield and volatiles composition during fast pyrolysis of food waste in the presence of hydrogen. Fuel Process Technol 210:106558. https://doi.org/10.1016/j.fuproc.2020.106558
50. Ly HV, Park JW, Kim SS, Hwang HT, Kim J, Woo HC (2020) Catalytic pyrolysis of bamboo in a bubbling fluidized-bed reactor with two different catalysts: HZSM-5 and red mud for upgrading bio-oil. Renew Energy 149:1434–1445. https://doi.org/10.1016/j.renene.2019.10.141
51. Xu R, Ferrante L, Briens C, Berruti F (2009) Flash pyrolysis of grape residues into biofuel in a bubbling fluid bed. J Anal Appl Pyrol 86(1):58–65. https://doi.org/10.1016/j.jaap.2009.04.005
52. Huang M, Xu JL, Ma ZQ, Yang YY, Zhou BL, Wu CL, Ye JW, Zhao C, Liu XH, Chen DY, Zhang WB (2021) Bio-BTX production from the shape selective catalytic fast pyrolysis of lignin using different zeolite catalysts: relevance between the chemical structure and the yield of bio-BTX. Fuel Process Technol 216:106792. https://doi.org/10.1016/j.fuproc.2021.106792
53. Wang WW, Lu YC, Xu KW, Wu K, Zhang ZS, Duan JH (2021) Experimental and simulated study on fluidization characteristics of particle shrinkage in a multi-chamber fluidized bed for biomass fast pyrolysis. Fuel Process Technol 216:106799. https://doi.org/10.1016/j.fuproc.2021.106799

54. Haydary J, Susa D, Gelinger V, Cacho F (2016) Pyrolysis of automobile shredder residue in a laboratory scale screw type reactor. J Environ Chem Eng 4(1):965–972. https://doi.org/10.1016/j.jece.2015.12.038
55. Pan R, Martins MF, Debenest G (2022) Optimization of oil production through ex-situ catalytic pyrolysis of waste polyethylene with activated carbon. Energy. https://doi.org/10.1016/j.energy.2022.123514
56. Wang CX, Lei HW, Qian MRO, Huo EG, Zhao YF, Zhang QF et al (2020) Application of highly stable biochar catalysts for efficient pyrolysis of plastics: a readily accessible potential solution to a global waste crisis. Sustain Energy Fuels 4:4614–4624. https://doi.org/10.1039/D0SE00652A
57. Pan R, Debenest G, Zanoni MA (2022) A robust two-dimensional model for the pyrolysis of plastic waste driven by self-sustaining smoldering. Process Saf Environ Prot 162:610–619. https://doi.org/10.1016/j.psep.2022.04.038
58. Pan R, Debenest G, Zanoni MA (2022) Numerical study of plastic waste pyrolysis driven by char smoldering. Process Saf Environ Prot 165:46–56. https://doi.org/10.1016/j.psep.2022.06.060
59. Aguado R, Olazar M, San Jose MJ, Gaisan B, Bilbao J (2002) Wax formation in the pyrolysis of polyolefins in a conical spouted bed reactor. Energ Fuel 16(6):1429–1437. https://doi.org/10.1021/ef020043w
60. Rodríguez-Luna L, Bustos-Martínez D, Valenzuela E (2021) Two-step pyrolysis for waste HDPE valorization. Process Saf Environ Prot 149:526–536. https://doi.org/10.1016/j.psep.2020.11.038
61. Sivagami K, Divyapriya G, Selvaraj R, Madhiyazhagan P, Sriram N, Nambi I (2021) Catalytic pyrolysis of polyolefin and multilayer packaging based waste plastics: a pilot scale study. Process Saf Environ Prot 149:497–506. https://doi.org/10.1016/j.psep.2020.10.038
62. Torres D, Jiang Y, Monsalve DAS, Leeke GA (2021) Chlorine removal from the pyrolysis of urban polyolefinic waste in a semi-batch reactor. J Environ Chem Eng 9(1):104920. https://doi.org/10.1016/j.jece.2020.104920
63. Pan R, Zan Y, Debenest G (2022) Oil production from waste polypropylene and polystyrene co-pyrolysis: interactions of temperature and carrier gas flow rate. J Environ Chem Eng. https://doi.org/10.1016/j.jece.2022.107555
64. Wang XB, Jin QM, Wang L, Bai S, Mikulcic H, Vujanovic M, Tan HZ (2019) Synergistic effect of biomass and polyurethane waste co-pyrolysis on soot formation at high temperatures. J Environ Manag 239:306–315. https://doi.org/10.1016/j.jenvman.2019.03.073
65. Pan RM, Martins MF, Debenest G (2021) Pyrolysis of waste polyethylene in a semi-batch reactor to produce liquid fuel: optimization of operating conditions. Energy Convers Manag 237:114114. https://doi.org/10.1016/j.enconman.2021.114114
66. Palos R, Gutierrez A, Vela FJ, Olazar M, Arandes JM, Bilbao J (2021) Waste refinery: the valorization of waste plastics and end-of-life tires in refinery units. A review. Energ Fuel 35(5):3529–3557. https://doi.org/10.1021/acs.energyfuels.0c03918
67. Harmon RE, SriBala G, Broadbelt LJ, Burnham AK (2021) Insight into polyethylene and polypropylene pyrolysis: global and mechanistic models. Energ Fuel 35(8):6765–6775. https://doi.org/10.1021/acs.energyfuels.1c00342